

Molecular Design of the Triphenylamine Substitution on Isoindigo-Based as Promising Hole Transport Materials for Perovskite Solar Cell

Natchaphon Ngueangam¹, Tanchanok Chaivisuthangkura²,
Nahathai Asawutmangkul², Benchawan Jityuti¹, and Pornthip Boonsri^{1*}

Received: 16 December 2022

Revised: 25 October 2022

Accepted: 26 December 2022

ABSTRACT

The performance of perovskite solar cells (PSCs) controlling the hole mobility is the fundamental importance. The development of novel hole transport materials (HTMs) with good stability, low cost and high hole mobility for PSCs has attracted much attention for researchers. In this work, new isoindigo-based HTMs substituted with two triphenylamine (TPA) with the donor-acceptor-donor (D-A-D) architecture, were designed computationally. The effect of π -extension influence on the charge transfer process was investigated by inserting of two vinyl groups between acceptor and donor parts (D- π -A- π -D). The correlation between electronic structure and hole transport properties of the designed HTMs was determined by tuning the connection between donor and acceptor. The ground state of the HTMs was fully optimized by DFT method at B3LYP/6-31G(d,p), and the excited state, absorption and emission properties of the HTMs were carried out by using the TD-DFT at cam-B3LYP/6-31G(d,p) in dichloromethane solvent based on the conductor-like polarizable continuum model (C-PCM). The calculated HOMO, LUMO and band gap values of the HTMs showed higher values than that of MAPbI₃ (perovskite). Hence, the charge distribution in HOMO and LUMO of our designed structures could qualitatively predicted the carrier injection and transportation in the PSCs. The adsorption spectra were broader, indicating that the proposed HTMs absorbed a large amount of visible light, which might impact the electron delocalization. This designed HTMs would have the potential for synthesis of new HTMs.

Keywords: Hole transport materials (HTMs), Isoindigo, Triphenylamine, Density functional theory (DFT)

¹ Department of Chemistry, Srinakharinwirot University, Sukhumvit 23, Bangkok 10110, Thailand.

² Patumwan Demonstration School, Srinakharinwirot University, Bangkok 10110, Thailand.

*Corresponding author, email: pornthipb@g.swu.ac.th

Introduction

Several global problems such as the lack of fossil fuels and increment of environmental pollution have led to several researches on clean and green alternative energy sources. The conversion of sunlight into electricity is one of the most promising renewable energy options for meeting future demand [1, 2]. Perovskite solar cells (PSCs) have attracted considerable interest among researchers in various photovoltaic technologies due to their many advantages such as low production costs, simple manufacturing process, and outstanding power conversion efficiencies (PCEs) [3, 4]. Generally, the structures of perovskite solar cell device consist of a perovskite absorber, an electron transporting material (ETM), a hole transport material (HTM), and a metallic counter electrode [5]. In such devices, HTM is one of the most crucial components for improving the PSCs performances [4, 6]. The HTM material should have qualifications such as: (1) high hole mobility, (2) appropriate energies of highest occupied molecular orbital (HOMO) and lowest unoccupied molecular orbital (LUMO) for effective hole injection and electron transport blocking, (3) high molecular stability, and (4) low synthetic costs [7-9]. Nowadays, 2,2',7,7'-tetrakis(N,N-di-p-methoxyphenylamine)-9,9'-spirobifluorene (spiro-OMeTAD) as the most popular HTM is applied in PSC devices [10, 11]. However, the high synthesis costs and low hole mobility of Spiro-OMeTAD limit its large-scale application [12]. Therefore, the development of new HTMs with high stability, low synthesis costs, and high hole mobility, is important to improve the performance of PSCs.

Isoidindigo, a symmetrical molecule composed of two indolin-2-one units, has been widely studied in solar-cell technologies [13, 14]. For example, Vatanparast et al. designed and investigated novel isoidindigo based donor-acceptor-donor (D-A-D) type HTMs for the PSCs, the results showed that the designed HTMs exhibited high hole mobility, and acceptable solubility and stability, which can be used as potential HTMs for the PSCs [15]. However, the isoidindigo based D-A-D type HTMs has been rarely reported for application in PSCs. Moreover, the effects of donor groups on the properties of isoidindigo based D-A-D type HTMs are rarely investigated. Thus, it is significant to select appropriate donor groups for the design of HTMs.

Triphenylamine is an important electron donor group that has been widely used to design HTMs. The HTMs based on triphenylamine are excellent hole transport materials due to their high hole mobility, good solubility in organic solvents, high thermal stability and low ionization potential [1, 16, 17]. Hence, the main purpose of this work is to design new isoidindigo-based HTMs with the D-A-D system and investigate the properties to examine suitability for use as HTMs in PSC devices. In the designed HTMs, isoidindigo is selected as the core acceptors and triphenylamine acts as the donor. Computational theory using density functional theory (DFT) and time-dependent density functional theory (TD-DFT) has been used to investigate the geometrical, electronic, optical properties, solubility and stability of the designed HTMs. In addition, the effects of π -extension on the properties of designed HTMs were examined by symmetrical insertion of two vinyl groups between isoidindigo core acceptor and triphenylamine units (D- π -A- π -D). From previous studied it confirmed that the substituents with the electron-donating group could improve the HOMO energy level of the molecules [15, 18, 19]. Therefore, the effect of difference

substitution groups at the para position of triphenylamine ring have been considered as the key properties for HTMs. The chemical structures of new isoindigo-based HTMs are shown in Figure 1.

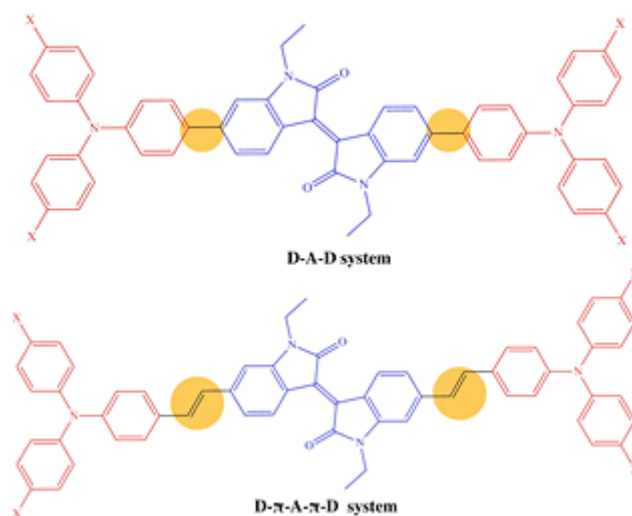


Figure 1 Chemical structures of the designed HTMs with X = N(Me)₂, NHMe, OMe, and OH substituents in the D-A-D and D- π -A- π -D systems.

Materials and Methods

All the calculations in this work were performed by the Gaussian 09 program package [20]. The energy levels and the frontier orbital distributions of designed HTMs were calculated using DFT method at B3LYP/6-31G(d,p) level [21, 22] with solvation effects in dichloromethane solution based on the conductor-like polarized continuum model (C-PCM) [23]. In order to investigate the optical properties of designed HTMs, the absorption and emission spectra were calculated using TD-DFT at cam-B3LYP/6-31G(d,p) level [24-26] in dichloromethane solution.

The adiabatic ionization potential (IP) and adiabatic electron affinity (EA) can be calculated from two following equations [9, 15]:

$$\text{IP} = (E_+) - (E_0) \quad (1)$$

$$\text{EA} = (E_0) - (E_-) \quad (2)$$

where E_+ , E_0 , and E_- illustrate the ground state energy values of the optimized cationic, neutral, and anionic states, respectively. All molecular structures were optimized using DFT method at B3LYP/6-31G(d,p) level. All molecular orbitals were analyzed and visualized by using Visual Molecular Dynamics (VMD) [27] and Gauss View 6 programs [20].

Results and Discussion

Electronic structures

In order to investigate the electronic properties of designed HTMs, the highest occupied molecular orbital (HOMO) and the lowest unoccupied molecular orbital (LUMO) were studied. More accurate prediction of HOMO energy level is essential to develop efficient HTMs [1]. However, the HOMO level gained from DFT calculations at B3LYP/6-31G(d,p) method is overestimated. Recently, Chi et al. has shown that the fitting HOMO levels ($\text{HOMO}_{\text{fitting}}$) achieved from DFT calculations (HOMO_{cal}) and the experimental HOMO level (HOMO_{exp}) of the 30 reference molecules showed that the linear equation and correlation coefficient ($R = 0.941$) was suitable to extrapolated to the HOMO_{exp} as shown in equation 3 [28].

$$\text{HOMO}_{\text{fitting}} = (1.107 \times \text{HOMO}_{\text{cal}}) - 0.118 \quad (3)$$

The $\text{HOMO}_{\text{fitting}}$ and HOMO_{cal} of the designed HTMs are reported in Table 1, showing that the calculations overestimate the HOMO levels.

Table 1 The fitting HOMO levels (eV) of the designed HTMs.

System	X	HOMO_{cal}	$\text{HOMO}_{\text{fitting}}$	Difference
D-A-D	OH	-4.77	-5.39	0.63
	OMe	-4.75	-5.38	0.63
	NHMe	-4.48	-5.08	0.60
	$\text{N}(\text{Me})_2$	-4.42	-5.02	0.59
D- π -A- π -D	OH	-4.67	-5.27	0.61
	OMe	-4.66	-5.28	0.63
	NHMe	-4.43	-5.03	0.59
	$\text{N}(\text{Me})_2$	-4.39	-4.97	0.59

Therefore, the fitting HOMO levels of designed HTMs in this work were calculated using this empirical equation, and the results are shown in Figure 2.

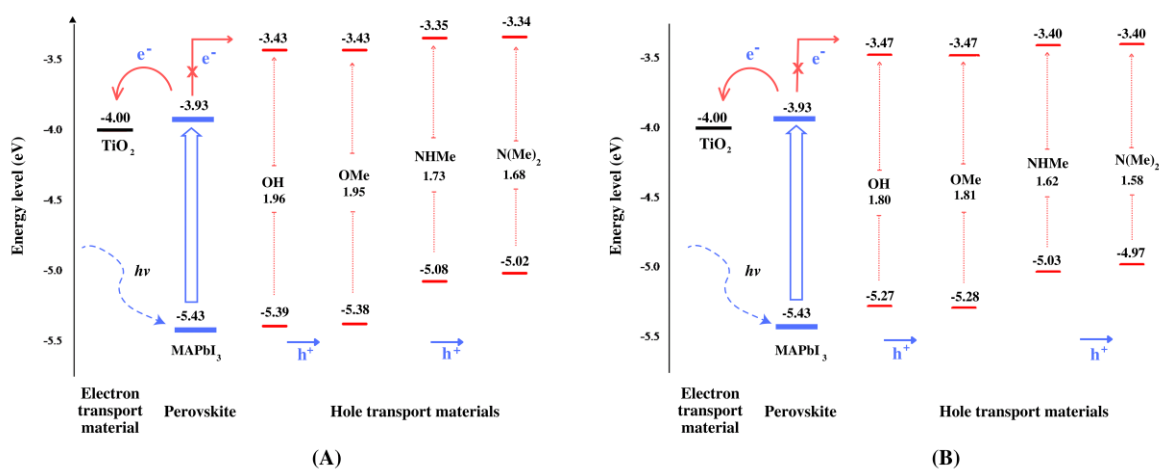


Figure 2 The energy levels diagram of the designed HTMs in (A) D-A-D and (B) D- π -A- π -D systems.

As a suitable HTM material in PSCs, the HOMO energy of the HTM should be higher than the valence band of the perovskite material (such as MAPbI₃, -5.43 eV) [15]. As shown in Figure 2, the HOMO energies of molecules with X = N(Me)₂, NHMe, OMe, and OH substituents in the D-A-D and D- π -A- π -D structure are located above the valence band of the MAPbI₃, which demonstrated that the hole can be effectively injected from the perovskite to the HTMs. For the LUMO energy, the LUMO energy levels should be higher than the conduction band of perovskite (such as MAPbI₃, -3.93 eV) to block the electron in perovskite back to electrodes [15]. The LUMO levels of designed HTMs in this work were calculated by equation 4.

$$\text{LUMO} = \text{HOMO}_{\text{fitting}} + \Delta E_{\text{HOMO-LUMO}} \quad (4)$$

where $\Delta E_{\text{HOMO-LUMO}}$ is the energy gap, which is calculated by DFT approaches. As displayed in Figure 2, the LUMO energy levels of molecules with X = N(Me)₂, NHMe, OMe, and OH substituents in the D-A-D and D- π -A- π -D structure are in the range between -2.86 to -2.75 eV. Comparing the LUMO energy of all designed HTMs with the conduction band of MAPbI₃, the LUMO energy levels of designed HTMs are higher than the conduction band of MAPbI₃. Thus, the backflow of electrons in perovskite to the electrode can be effectively blocked.

However, the charge mobility of the molecule depends upon the planarity and rigidity, such as bond lengths and torsion angles. Since all the designed structure was almost planar, particularly in the D- π -A- π -D system, adding the π -linker results in a planar and rigid molecular structure as can be clearly explained in Figure 3 and 4.

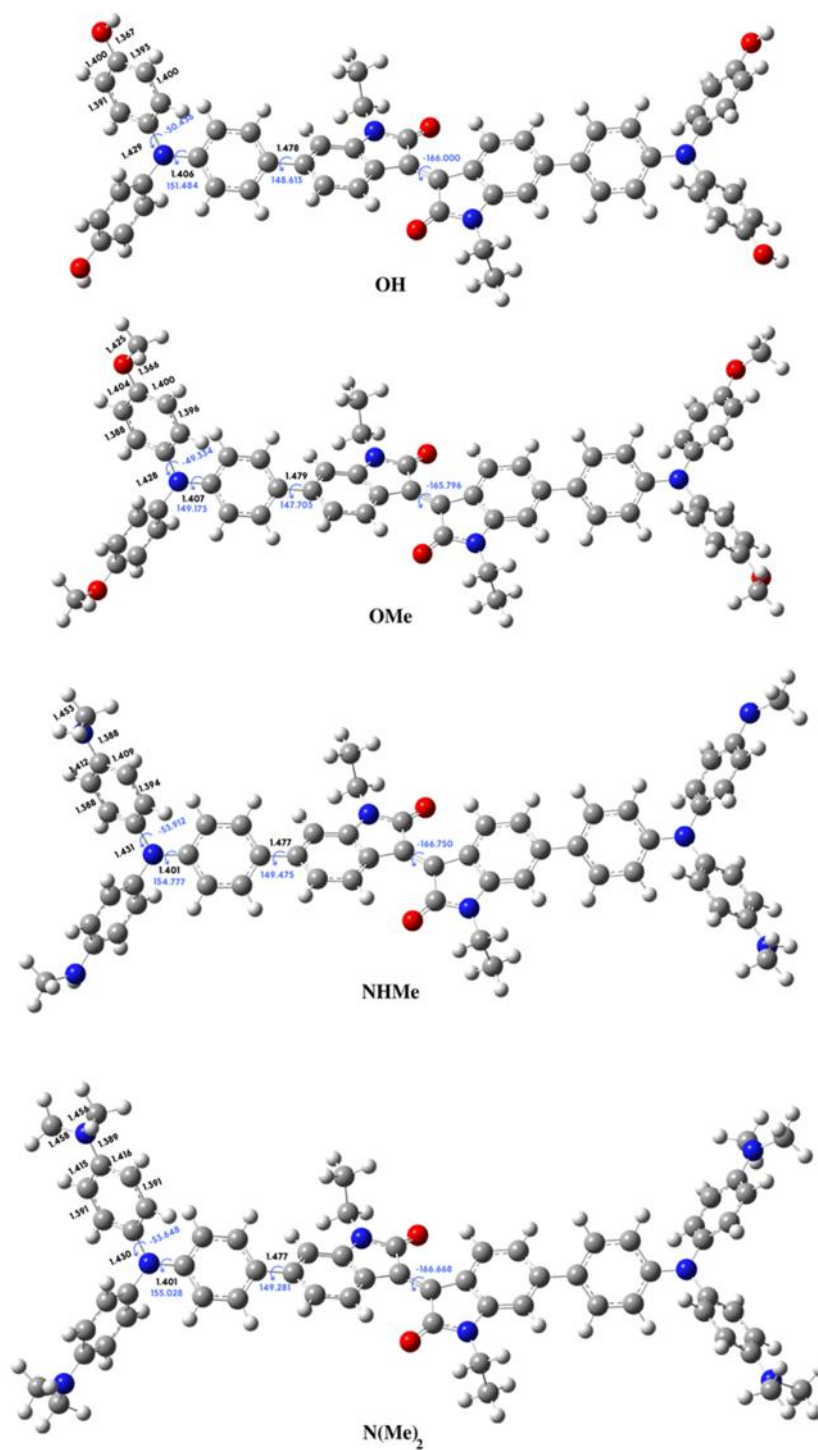


Figure 3 Structural properties of the designed HTMs in D-A-D systems. Bond lengths (black) are in Å and torsion angle (blue) are in degree.

Furthermore, the energy and distribution pattern of the frontier molecular orbitals (FMOs) plays an important role in charge transport. As display in Figure 5, the HOMOs of designed HTMs are generally delocalized throughout the whole molecule, while the LUMOs are mainly located on the isoindigo unit. The more delocalized distribution of the HOMOs can enhance the charge transfer efficiency. Thus, these designed isoindigo based HTMs would have the potential to be used as hole-transporting materials in PSCs.

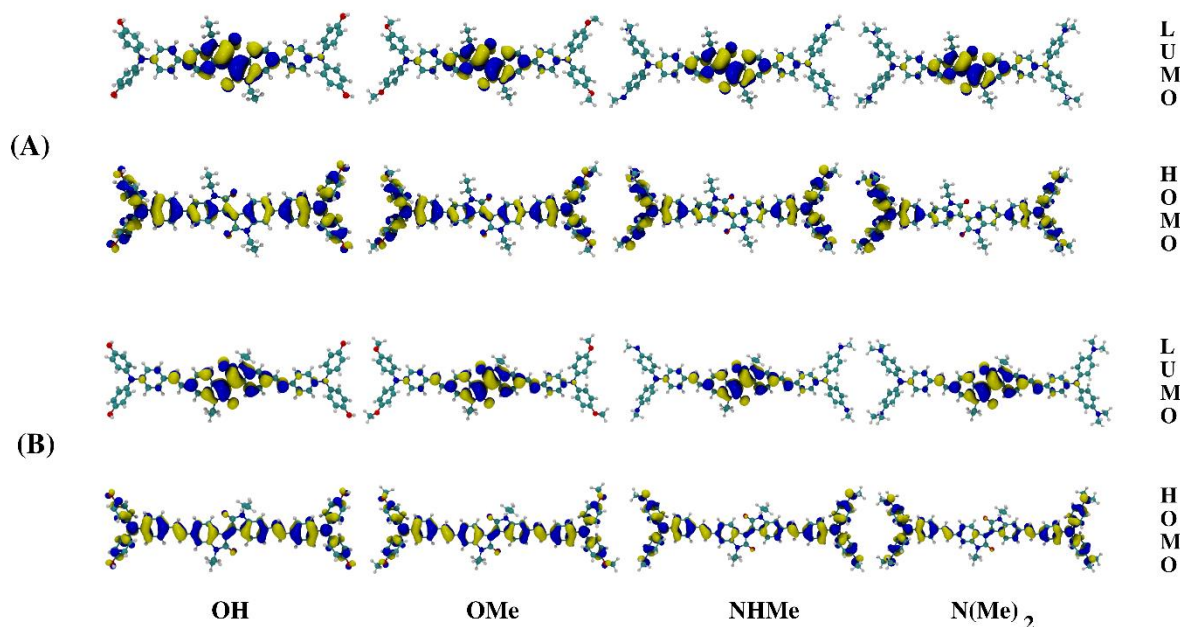


Figure 5 The frontier molecule orbitals of the designed HTMs in (A) D-A-D and (B) D- π -A- π -D systems.

Optical properties

To characterize the optical properties, the absorption and emission spectra of designed HTMs in dichloromethane solvent were calculated using TD-DFT at cam-B3LYP/6-31G(d,p) level. The simulated absorption spectra of designed HTMs are displayed in Figure 6, and the optical parameters including the wavelength of maximum absorbance (λ_{abs}), maximum emission (λ_{em}), and Stokes shift are presented in Table 2.

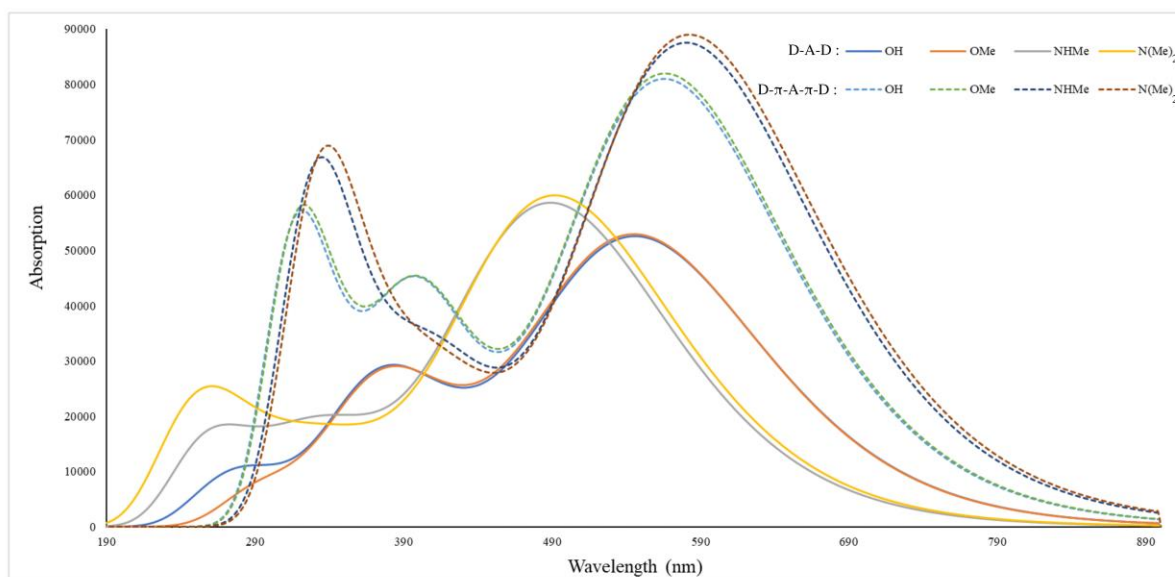


Figure 6 Absorption spectra of the designed HTMs in D-A-D and D- π -A- π -D systems.

Table 2 The maximum absorbance wavelength (λ_{abs}), the absorption oscillator strength (f), the maximum emission wavelength (λ_{em}), and Stokes shift of the designed HTMs.

System	X	λ_{abs} (nm)	f	λ_{em} (nm)	Stokes shift (nm)
D-A-D	OH	518.05	1.2886	707.22	189.17
	OMe	517.49	1.2950	706.93	189.44
	NHMe	531.34	1.4363	720.42	189.08
	N(Me) ₂	533.96	1.4692	723.72	198.76
D- π -A- π -D	OH	566.18	1.9941	753.84	187.66
	OMe	566.76	2.0170	752.63	185.87
	NHMe	581.04	2.1522	765.44	184.40
	N(Me) ₂	583.32	2.1879	767.87	184.55

According to these results, the maximum absorption (λ_{abs}) of D-A-D typed HTMs is in the range between 517 and 534 nm. However, increasing the π -conjugation of D- π -A- π -D system leads to more red shifts by 48 - 50 nm in the absorption spectra compared with that of D-A-D system. The results illustrate that the designed isoindigo based HTMs in D-A-D and D- π -A- π -D system can absorb a significant amount of visible light, and hence, they can be considered as HTMs for the PSCs. The Stokes shift can be determined from the difference of maximum absorbance (λ_{abs}) and maximum emission (λ_{em}). As listed in Table 2, the Stokes shifts of the designed HTMs are in the range between 184 and 199 nm. The D- π -A- π -D system display the larger Stokes shifts than the D-A-D system. This large

Stokes shift values for designed HTMs is consequence of a large geometric structure changes from ground-state to excited-state level, which can be helpful for the pore-filling of the designed HTMs.

Solubility and stability

Besides the electronic and optical properties of the designed HTMs, the solubility and stability of the designed HTMs are also evaluated. The solubility of HTMs in organic solvents can be estimated by calculation of solvation free energy (ΔG_{sol}), using equation (5), which is defined by the following relationship [15]:

$$\Delta G_{\text{sol}} = G_{\text{sol}} - G_{\text{gas}} \quad (5)$$

where G_{sol} and G_{gas} represent the free energies of the designed HTMs in solvent and gas phases, respectively. The calculated solvation free energies of all designed HTMs are displayed in Table 3. The values of the solvation free energies in all molecules are negative, indicating that the solvation is a spontaneous process. Moreover, the solvation free energies of designed HTMs in D- π -A- π -D structure are more negative than that of D-A-D structure, leading to the better solubility in dichloromethane solvent. It indicated that the insertion of a vinyl bond between the donor and isoindigo-core acceptor increases the solubility for the HTMs.

The stability of photo-oxidation of HTMs can be investigated from which molecule can give the higher ionization potential (IP) value. As reported in Table 3, the IP values of the designed HTMs are in the range between 4.73 and 5.35 eV. The IP values decrease with increasing the electron-donating characteristic of the side chains on triphenylamine moiety. Moreover, the substitution with OH and OMe groups illustrated the higher IP values which revealed as the most stable HTMs against photo-induced oxidation. For the electron affinity (EA), the lower values indicate that the HTMs can block electron injection from PSCs [7] in the opposite case, high EA values characteristic of semiconductor materials [29]. All the designed HTM showed values of derivatives of NHMe and N(Me)₂, which presented the lower values. Thus, the NHMe and N(Me)₂ groups can increase the electron-blocking ability, which has the same conclusions as the energy levels analysis.

In order to investigate the molecular stability of the designed HTMs, the absolute hardness (η) is calculated from the relationship between the IP and the EA as shown in equation 6, and the results are listed in Table 3. The absolute hardness of designed HTMs is defined by the following formula [17, 28]:

$$\eta = (\text{IP} - \text{EA})/2 \quad (6)$$

The larger absolute hardness values indicate a high stability of the material. As presented in Table 3, the absolute hardness values of designed HTMs in D-A-D structure are higher than that of D- π -A- π -D structure, indicating that the stability of the D-A-D typed HTMs is better than that of the D- π -A- π -D typed HTMs. Moreover, the stability of the designed HTMs decreases with increasing the electron-donating characteristic of the side chains on triphenylamine moiety. Among them, the substitution with OH group is the most stable compound.

Table 3 Solvation free energy (ΔG_{sol}), adiabatic ionization potential (IP), adiabatic electron affinity (EA), and absolute hardness (η) of the designed HTMs.

Parameters	D-A-D systems				D- π -A- π -D systems			
	OH	OMe	NHMe	N(Me) ₂	OH	OMe	NHMe	N(Me) ₂
ΔG_{sol} (kcal/mol)	- 18.62	-14.16	-17.23	-14.80	-20.21	-15.65	-18.74	-16.31
IP (eV)	5.35	5.28	4.86	4.79	5.19	5.13	4.80	4.83
EA (eV)	1.62	1.59	1.45	1.44	1.75	1.72	1.59	1.58
η (eV)	1.87	1.84	1.71	1.67	1.72	1.70	1.60	1.58

Additionally, the electrostatic surface potential (ESP) has been used to estimate the molecular stability of designed HTMs [28]. The calculated ESPs maps for all designed HTMs are shown in Figure 7. The regions of negative charge and positive charge are shown in red and blue colors, respectively. The ESP maps show that the negative charges are mostly distributed on the center of isoindigo rings, while the positive charges are mainly positioned on triphenylamine moiety. The potential of negative regions on the isoindigo core are enlarged and reinforced by increasing the electron donating character of the side chains on the triphenylamine moiety, which render the oxidation easy and reduces the molecular stability. These results corresponded to the calculation data obtained from the absolute hardness.

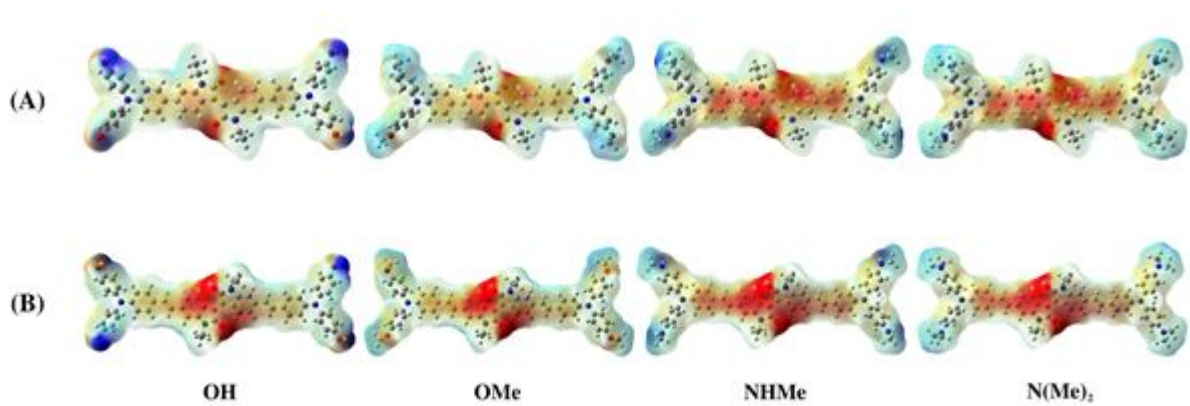


Figure 7 Electrostatic surface potentials of the designed HTMs in (A) D-A-D and (B) D- π -A- π -D systems.

Conclusions

In this work, novel hole transport material (HTM) with the donor-acceptor-donor (D-A-D) and D- π -A- π -D configuration are designed based on isoindigo as the core acceptors and triphenylamine acts as the donor. The electronic structures and optical properties of the designed HTMs were investigated using density functional theory (DFT) and time-dependent density functional theory (TD-DFT) methods. Our results showed that the HOMO energy levels of all molecules in the D-A-D and D- π -A- π -D

structure were higher than the valence band of the MAPbI₃ perovskite, which indicated that the hole can be effectively injected from the perovskite to the HTMs. The LUMO energy levels of all molecules were located above the conduction band of MAPbI₃ perovskite, which indicated that the backflow of electrons in perovskite to the electrode can be effectively blocked. The solubility of the designed HTMs showed negative energy values which indicated that the solvation was a spontaneous process. Thus, our investigation discovers that the introduction of the vinyl group will strengthen the solubility of the HTMs. The stability of photo-oxidation of HTMs because of higher ionization potential (IP) value, indicated that the addition of OH and NHMe groups revealed the most stable. Adding a replacement NHMe and N(Me)₂ groups can increase the electron-blocking ability, which has the same conclusions as the energy levels analysis. The stability of the absolute hardness (η) and electrostatic surface potential (ESP) calculations revealed that the stability of the HTMs decreased with an increase in the electron-donating character of the side chains on the triphenylamine moiety, which renders the oxidation easy and reduces the molecular stability and corresponding to the calculation data obtained from the absolute hardness. The development of isoindigo based HTMs might be beneficial for the synthesis of novel HTMs, according to the findings of this computational study.

Acknowledgements

Department of Chemistry, Faculty of Science, Srinakharinwirot University are gratefully acknowledged for providing research facilities. Finally, National e-Science Infrastructure Consortium are thankfully acknowledged for providing computing resources that have partly contributed to the research results reported within this paper.

References

1. Rezaei F, Mohajeri M. Molecular designing of triphenylamine-based hole-transporting materials for perovskite solar cells. *Sol Energy*. 2021;221:536-44.
2. Darling SB, You F, Veselka T, Velosa A. Assumptions and the levelized cost of energy for photovoltaics. *Energy Environ Sci*. 2011;4:3133-9.
3. Kumar A, Singh S. Computational simulation of metal doped lead-free double perovskite (Cs₂AgBi_{0.75}Sb_{0.25}Br₆) solar cell using solar cell capacitance simulator. *Mater Today: Proc*. 2021;44:2215-22.
4. Liu H, He B, Lu H, Tang R, Wu F, Zhong C, et al. Carbazole-based D–A type hole transport materials to enhance the performance of perovskite solar cells. *Sustain Energy Fuels*. 2022;6:371-6.
5. Ye X, Zhao X, Li Q, Ma Y, Song W, Quan YY, et al. Effect of the acceptor and alkyl length in benzotriazole-based donor-acceptor-donor type hole transport materials on the photovoltaic performance of PSCs. *Dyes Pigm*. 2019;164:407-16.

6. Liu P, Xu B, Hua Y, Cheng M, Aitola K, Sveinbjörnsson K, et al. Design, synthesis and application of a π -conjugated, non-spiro molecular alternative as hole-transport material for highly efficient dye-sensitized solar cells and perovskite solar cells. *J Power Sources*. 2017;344:11-4.
7. Wang Q, Zeng Z, Li Y, Chen X. Efficient strategies for improving the performance of EDOT derivatives and TPA derivatives-based hole transport materials for perovskite solar cells. *Sol Energy*. 2020;208:10-9.
8. Sun ZZ, Hao M, Feng S, Ding WL, Peng XL. Boosting the performance of D–A–D type hole-transporting materials for perovskite solar cells via tuning the acceptor group. *New J Chem*. 2020;44:15244-50.
9. Vatanparast M, Shariatinia Z. Efficient hole transport materials based on naphthyridine core designed for application in perovskite solar photovoltaics. *J Mol Graph Model*. 2022;117:108292.
10. Zhang Y, Li Y, Chen C, Wang L, Zhang J. Design new hole transport materials for efficient perovskite solar cells by suitable combination of donor and core groups. *Org Electron*. 2017;49:255-61.
11. Liu H, Sun H, Chen Q, Wu F, Liu X. Two simple hole-transporting materials for perovskite solar cells: A DFT calculation and experimental study. *Appl Surf Sci*. 2022;604:154603.
12. Tu B, Wang Y, Chen W, Liu B, Feng X, Zhu Y, et al. Side-chain engineering of donor–acceptor conjugated small molecules as dopant-free hole-transport materials for efficient normal planar perovskite solar cells. *ACS Appl Mater Interfaces*. 2019;11:48556-63.
13. Wang E, Ma Z, Zhang Z, Henriksson P, Inganäs O, Zhang F, et al. An isoindigo-based low band gap polymer for efficient polymer solar cells with high photo-voltage. *Chem Commun*. 2011;47:4908-10.
14. Khalili G, McCosker PM, Clark T, Keller PA. Synthesis and density functional theory studies of aziranyl and oxiranyl functionalized isoindigo and (3Z,3'Z)-3,3'-(ethane-1,2-diylidene)bis(indolin-2-one) derivatives. *Molecules*. 2019;24(20):3649.
15. Vatanparast M, Shariatinia Z. Isoindigo derivatives as promising hole transport materials for perovskite solar cells. *Sol Energy*. 2021;230:260-8.
16. Gapol MAB, Kim DH. Novel adamantane-based hole transport materials for perovskite solar cells: a computational approach. *Phys Chem Chem Phys*. 2019;21:3857-67.
17. Xu YL, Ding WL, Sun ZZ. How to design more efficient hole-transporting materials for perovskite solar cells? Rational tailoring of the triphenylamine-based electron donor. *Nanoscale*. 2018;10:20329-38.
18. Hansch C, Leo A, Taft RW. A Survey of Hammett Substituent Constants and Resonance and Field Parameters. *Chem Rev*. 1991;91(2):165-95.
19. Stępien BT, Cyranski MK, Krygowski TM. Aromaticity strongly affected by substituents in fulvene and heptafulvene as a new method of estimating the resonance effect. *Chem Phys Lett*. 2001;350:537-42.

20. Frisch MJ, Trucks GW, Schlegel HB, Scuseria GE, Robb MA, Cheeseman JR, et al. Gaussian 09, Revision C.01. Wallingford CT. 2010.
21. Johnson BG, Frisch MJ. Analytic second derivatives of the gradient-corrected density functional energy. *Chem Phys Lett.* 1993;216(1):133-40.
22. Pople JA, Gill PMW, Johnson BG, Kohn—Sham density-functional theory within a finite basis set. *Chem Phys Lett.* 1992;199(6):557-60.
23. Cossi M, Rega N, Scalmani G, Barone V. Energies, structures, and electronic properties of molecules in solution with the C-PCM solvation model. *J Comput Chem.* 2003;24(6):669-81.
24. Gross EKV, Kohn W. Time-dependent density-functional theory. *Adv Quantum Chem.* 1990;21:255-91.
25. Runge E, Gross EKV. Density-functional theory for time-dependent systems. *Phys Rev Lett.* 1984;52(12):997-1000.
26. Yanai T, Tew DP, Handy NC. A new hybrid exchange–correlation functional using the Coulomb-attenuating method (CAM-B3LYP). *Chem Phys Lett.* 2004;393(1):51-7.
27. Humphrey W, Dalke A, Schulten K. VMD: Visual molecular dynamics. *J Mol Grap.* 1996;14(1):33-8.
28. Chi WJ, Li QS, Li ZS. Exploring the electrochemical properties of hole transport materials with spiro-cores for efficient perovskite solar cells from first-principles. *Nanoscale.* 2016;8:6146-54.
29. Chai S, Wen SH, Huang JD, Han KL. Density functional theory study on electron and hole transport properties of organic pentacene derivatives with electron-withdrawing substituent. *J Comput Chem.* 2011;32:3218-25.